Journal of Alloys and Compounds 489 (2010) 600–604

Contents lists available at ScienceDirect

Journal of Alloys and Compounds

journal homepage: www.elsevier.com/locate/jallcom

Synthesis and characterization of pure nanocrystalline magnesium aluminate spinel powder

F. Tavangarian*, R. Emadi

Department of Materials Engineering, Isfahan University of Technology (IUT), Isfahan 84156-83111, Iran

ARTICLE INFO

Article history:
Received 22 August 2009
Received in revised form
16 September 2009
Accepted 19 September 2009
Available online 25 September 2009

Keywords:
Spinel
Ceramics
Mechanical activation
Cold crushing strength
Nanostructured materials

ABSTRACT

Synthesis of nanocrystalline magnesium aluminate spinel ($MgAl_2O_4$) by mechanical activation of a powder mixture containing Al_2O_3 and $MgCO_3$ with subsequent annealing was investigated. Simultaneous thermal analysis (STA), X-ray diffraction (XRD), and scanning electron microscopy (SEM) techniques were utilized to characterize the as-milled and annealed samples. Results showed that pure nanocrystalline spinel could be fabricated completely by 5 h of mechanical activation with subsequent annealing at 1200 °C for 1 h with a crystallite size of about 45 nm. Further milling had no significant effects on structure or phase composition of spinel phase after subsequent annealing. The nanocrystalline spinel powder obtained after 60 h of milling and subsequent annealing at 1200 °C for 1 h had a crystallite size of about 25 nm according to Williamson–Hall approach and particle sizes smaller than 200 nm. Enhanced mechanical properties were observed in samples prepared from the powder mixture and milled for a longer period.

1. Introduction

Nanocrystalline materials with an average crystalline size of a few nanometers have been of much interest to many investigators [1–3]. Nanomaterials exhibit increased strength/hardness, enhanced diffusivity, improved ductility/toughness, reduced density, reduced elastic modulus, increased specific heat, etc. They have high potentials for use in structural and device applications in which enhanced mechanical and physical properties are required [4,5].

Magnesium aluminate spinel ($MgAl_2O_4$) is one of the best known and widely used materials. It develops high strength at both elevated and normal temperatures which, combined with the fact that it has no phase transition up to the melting temperature (2135 °C), makes it an excellent refractory material [6]. Also due to its good thermal shock resistance, high chemical inertness in both acidic and basic environments, and excellent optical and dielectric properties, spinel is widely used in the metallurgical, electrochemical, and chemical industrial fields [7–9]. Moreover, spinel has found applications in dentistry [10], catalyst supports [11], humidity sensors [12], reinforcing fibers [13], photoluminescent materials [14], nuclear technology [15], and ceramic pigments [16].

Several synthetic methods have been used to synthesize spinel powder that include the precipitation route [17], the aerosol method [18], the citrate–nitrate route [19,20], sol–gel of double or semi-alkoxides [21,22], spray drying [23], freeze-drying [24], organic gel-assisted citrate process [25]. The traditional method of synthesizing this material is the ceramic one in which the reaction in the solid phase takes place at high temperatures (>1400–1500 °C) between oxides (or hydroxides or salts) of aluminium and magnesium [26]. This process has some disadvantages, the most important being low surface area and chemical inhomogeneity. Mechanical activation is an efficient method to improve the contact and interaction of the reactants by the milling process, which increases the chemical homogeneity of the product and reduces the severity of thermal treatment [27]. Although, synthesis of spinel by a combination of mechanochemical treatment of aluminium hydroxide (gibbsite) and magnesium hydroxide (brucite) powder mixture with subsequent heat treatment has been previously investigated [28], the crystallite size of the final product was not in the nano-range, requiring heat treatment at temperatures between 1400 and 1600 °C. The purpose of the present work was to develop an easy method for synthesizing pure nanocrystalline spinel powder from alumina (Al_2O_3) and magnesite ($MgCO_3$) through mechanical activation with subsequent annealing.

2. Experimental procedures

2.1. Powder preparation

The powders of alumina (Al_2O_3) (99% purity, Merck) and magnesium carbonate ($MgCO_3$) (98% purity, Aldrich) were used as raw materials. $MgCO_3$ is a better choice than MgO since it is less hygroscopic and because on decomposition at high temperatures of 600–900 °C, a fine grained MgO with a high surface area and reactivity

* Corresponding author. Tel.: +98 311 3915725; fax: +98 311 3912752.
E-mail address: f.tavangarian@yahoo.com (F. Tavangarian).

0925-8388/$ – see front matter © 2009 Elsevier B.V. All rights reserved.
doi:10.1016/j.jallcom.2009.09.120

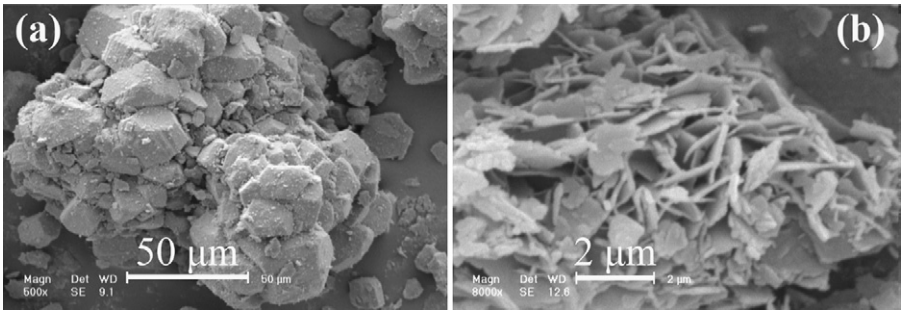

Fig. 1. Morphology of (a) Al_2O_3 and (b) $MgCO_3$ powders before milling.

should result [29]. Fig. 1 shows the morphology of the initial powder agglomerates. The alumina powder has an angular shape with a mean agglomerate diameter of about 100 μm. $MgCO_3$ powder has a lamellar shape with a mean agglomerate size of about 10 μm. The agglomerate size of powders was determined using scanning electron microscopy (SEM). Several micrographs were used for agglomerate size measurement and the average value was reported. $MgCO_3$ and alumina powders with a molar ratio of 1:1 were mixed to yield a single phase spinel. The powder mixture was mechanically activated in a planetary ball mill (Fritsch P7 type) under ambient conditions. The milling media consisted of a corundum container with corundum balls (10 balls 10 mm in diameter). In all milling runs, the ball-to-powder weight ratio was 10:1 and the rotational speed of the main disc was 500 rpm. Heat treatment of the ball milled powders was carried out at 1200 °C for 1 h in air.

2.2. Preparation of bulk sample

To evaluate the effect of milling time on the cold crushing strength (CCS) of the prepared bulk samples, the 2–60 h milled powders were uniaxially pressed into pellets in a hardened steel mould at a pressure of 500 MPa. Pellets of 12 mm in diameter and 12 mm long were prepared for the determination of CCS according to the ASTM standard (C0020-00R05).

Sintering of green bodies was carried out in a programmable resistance furnace. To prevent the fracture of bodies during sintering, the samples were heated up to 600 °C in the first stage at a heating rate of 2 °C/min. In this situation, hydration water and CO_2 were liberated more slowly from the pores. The specimens were then heated up to 1200 °C at a heating rate of 10 °C/min. After retention for 1 h at 1200 °C, the specimens were cooled down to 600 °C at a rate of 50 °C/min to avoid grain growth. The samples were then cooled down to ambient temperature at a rate of 10 °C/min.

2.3. Characterization

Phase transformation during ball milling with subsequent annealing was investigated by X-ray diffractometry (XRD) using a Philips X'PERT MPD diffractometer with Cu Kα radiation (λ = 0.154056 nm). The XRD traces were recorded in the 2θ range of 20–80° (step size of 0.04° and time per step of 1 s). The Williamson–Hall method was used to estimate the crystallite size of the spinel powder [30]:

$$\beta \cos\theta = \frac{K\lambda}{D} + \varepsilon \sin\theta \quad (1)$$

where θ is the Bragg diffraction angle, D is the crystallite size, ε is the average internal strain, λ is the wavelength of the radiation used, β is the diffraction peak width at half maximum intensity, and K is the Scherrer constant (0.91) [30].

The morphology of powder particles was studied by scanning electron microscopy (SEM) in a Philips XL30 at an acceleration voltage of 30 kV. Image analysis was used to measure spinel powder particles. Differential thermal analysis (DTA) was performed on as-milled powders in order to observe any exothermic peaks which may indicate crystallization temperatures of the spinel. Weight losses during temperature rise were measured using thermogravimetric analysis (TG) at temperatures ranging from room temperature to as high as 1200 °C in air and at a heating rate of 10 °C/min. CCS was measured by a Hydraulic Testing Machine type Amsler model D3010/2E.

3. Results and discussion

3.1. Thermal analysis

Fig. 2 shows the DTA and TG curves of powder after 5 min of milling. As can be seen, the two endothermic bands observed at 290 and 515 °C are attributed to dehydration and magnesite decomposition, respectively [3]. At 1040 °C, a small exothermic effect was detected associated with the nucleation and formation of spinel by reaction between alumina and periclase (MgO), as reported by Sainz et al. [31]. The weight loss of the ball milled powder occurred in three main stages. The first stage occurred at a temperature below 350 °C probably due to the loss of water to hydration. The second stage of weight loss took place below 700 °C due to the decomposition of magnesium carbonate and crystallization of MgO. Finally, at temperature around 1050 °C, the third stage occurred due to the formation of spinel structure [31]. There was no further significant weight loss above this temperature. So, heat treatment for preparing spinel was performed at above 1050 °C.

3.2. XRD analysis

Alumina and magnesite reaction rate depends on the contact area between the reactants (depending on their surface area), the nucleation velocity of the final product (subordinated to the structural similarity between the product and, at least, one reactant), and the diffusion rate of the ions through the phases of reactants and products (influenced by the particle size, the mixing degree, and the intimate contact of the reactants). With respect to the nucleation velocity of the $MgAl_2O_4$, it must be noted that it is favored due to the structural similarity between the spinel and alumina, since Al_2O_3 can be considered as a defective spinel [32]. Considering these observations, $MgCO_3$ and Al_2O_3 were mechanically activated. Fig. 3 shows the XRD patterns of prepared powders after different mechanical activation times. It can be seen that the starting materials of alumina (XRD JCPDS data file No. 01-1308) and $MgCO_3$ (XRD JCPDS data file No. 18-0769) remained after 5 min of mechanical activation. After milling for 10 h, the XRD pattern peaks of $MgCO_3$ disappeared. $MgCO_3$ particles got finer and partially decomposed during ball milling, indicating that mechanical activation gradually creates the state in which the mixtures are amorphous [33]. The changes in diffraction line intensities of basic $MgCO_3$ are also faster in comparison to pure, mechanically activated basic $MgCO_3$ [34]. But even after 60 h of milling, the XRD pattern peaks of Al_2O_3 still persisted. Increasing the milling time up to 60 h led to the broadening of XRD peaks and to a significant decrease in their intensity as a result of refinement of crystallite size and enhancement of lattice

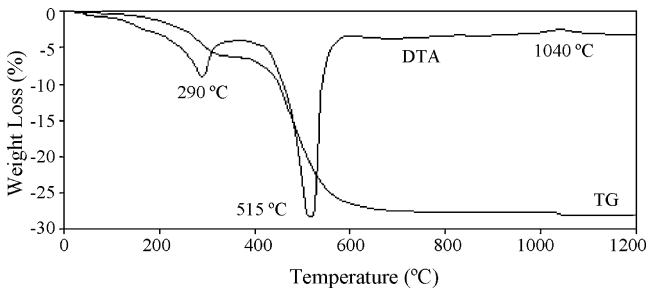

Fig. 2. DTA and TG curves of powder after 5 min milling.

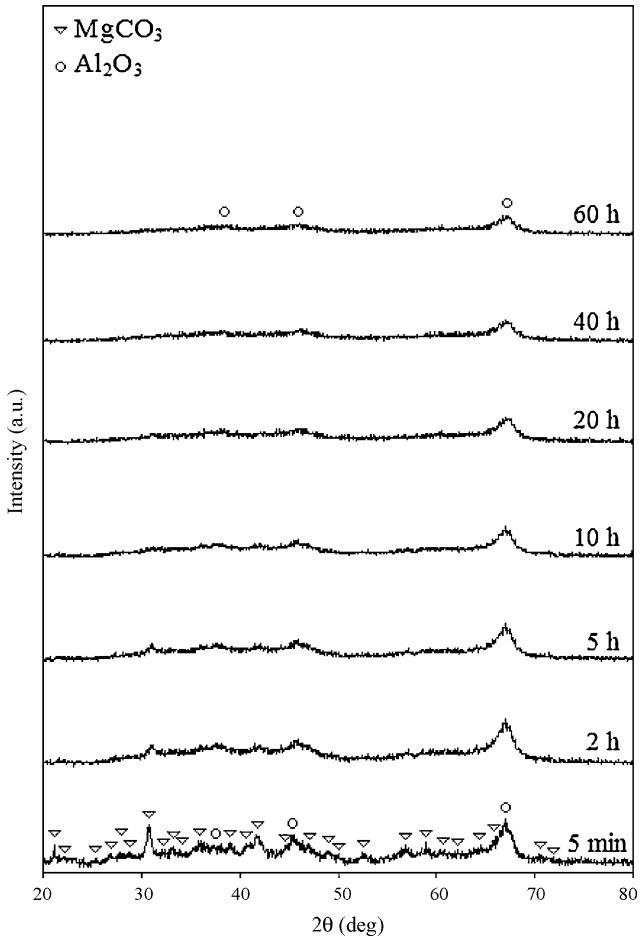

Fig. 3. X-ray diffraction patterns of starting materials after various mechanical activation times.

strain. No new crystalline phase was observed in the XRD patterns even after 60 h of mechanical activation.

To check the possibility of spinel phase formation during subsequent heat treatment, the milled powders were annealed at 1200 °C for 1 h. Fig. 4a shows the XRD patterns of obtained powders after mechanical activation for various periods of time with subsequent annealing at 1200 °C for 1 h. The XRD pattern of the sample milled for 5 min corresponds to those of alumina (XRD JCPDS data file No. 10-0173), periclase (XRD JCPDS data file No. 43-1022), and spinel (XRD JCPDS data file No. 21-1159) phases after subsequent annealing. In the first stage, magnesite is decomposed according to the following reaction:

$$MgCO_3 \rightarrow MgO + CO_2 \qquad \Delta G_{1200\,^\circ C} = -141.896\ \text{kJ/(mol K)} \quad (2)$$

After this stage, the produced MgO reacts with Al_2O_3 to form spinel:

$$MgO + Al_2O_3 \rightarrow MgAl_2O_4 \qquad \Delta H_{1200\,^\circ C} = -47.201\ \text{kJ/(mol K)}$$

$$\Delta G_{1200\,^\circ C} = -37.411\ \text{kJ/(mol K)} \quad (3)$$

The negative values of ΔG and ΔH at 1200 °C for reaction (3) indicate that the spinel reaction may occur at 1200 °C and that it is exothermic. Schacht [35] proposed that at the interface between particles of MgO and Al_2O_3, small crystals with the spinel stoichiometry and structure are nucleated relatively easily on the surfaces of either MgO or Al_2O_3 grains. Once these initial spinel layers form, subsequent growth or thickening of the spinel product becomes much more difficult because, effectively, the two reactants, MgO and Al_2O_3, are no longer in contact but are separated by a rather impenetrable spinel layer. To continue the reaction, a complex counter-diffusion process is thus required in which Mg^{2+} ions diffuse away from, and Al^{3+} ions diffuse toward, the MgO–$MgAl_2O_4$ interface and vice versa for the $MgAl_2O_4$–Al_2O_3 interface.

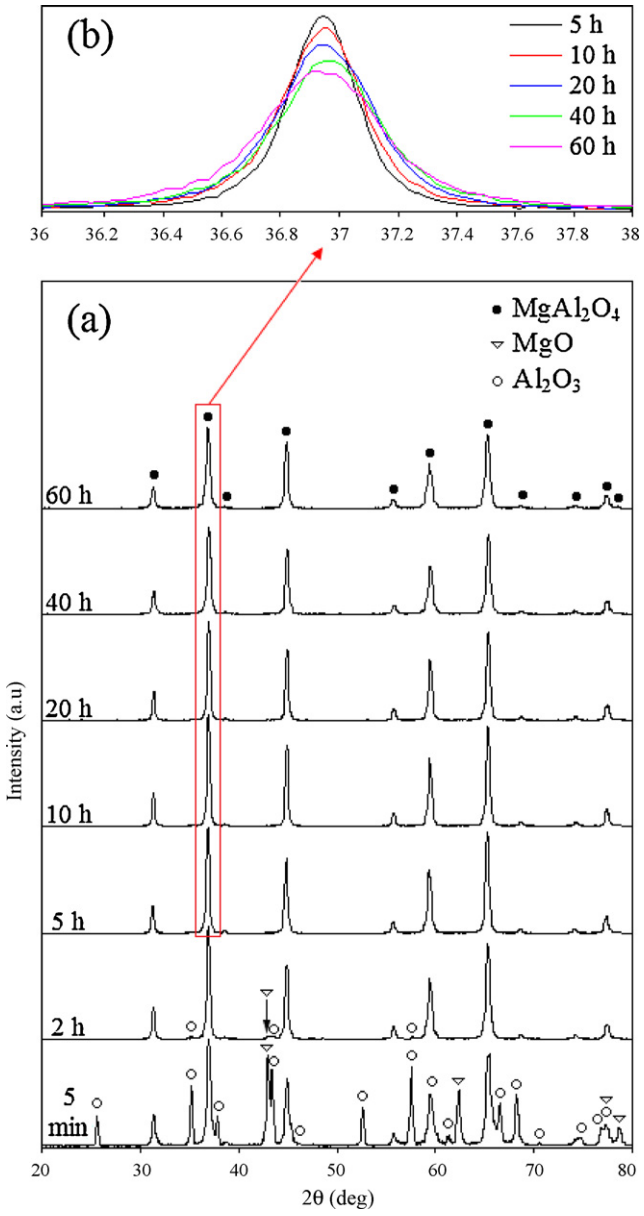

Fig. 4. (a) XRD patterns of powders obtained after mechanical activation for various periods of time with subsequent annealing at 1200 °C for 1 h and (b) decrease in the intensity of XRD peaks with increasing milling time.

In this situation, spinel formation is particularly slow because ions such as Mg^{2+} and Al^{3+} diffuse slowly. Defects are required, particularly vacant sites into which adjacent ions can hop. This can be promoted by dynamically maintained high reaction interface areas as well as the short-circuit diffusion path provided by the large number of defects such as dislocations and grain boundaries induced during ball milling.

Detailed analysis of the changes in the MgO diffraction line intensities is one parameter that can be used for describing the reaction progress. As can be seen, in the powder milled for 2 h, the fraction of spinel phase increased to a great extent while traces of MgO and Al_2O_3 were observed after the subsequent annealing. Fast disappearance of MgO diffraction lines is the result of the effect of mechanical activation on the reaction rate as a result of better reactivity of initial materials. Mechanical activation increases the

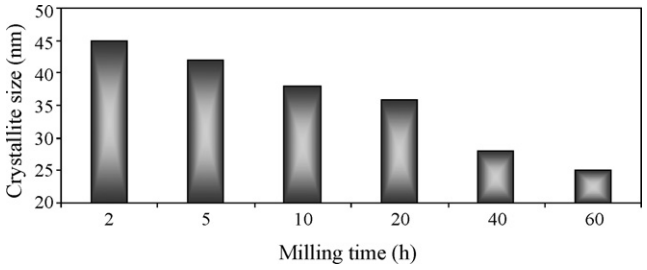

Fig. 5. Crystallite sizes of the spinel phase as a function of period of mechanical activation after subsequent annealing at 1200 °C for 1 h.

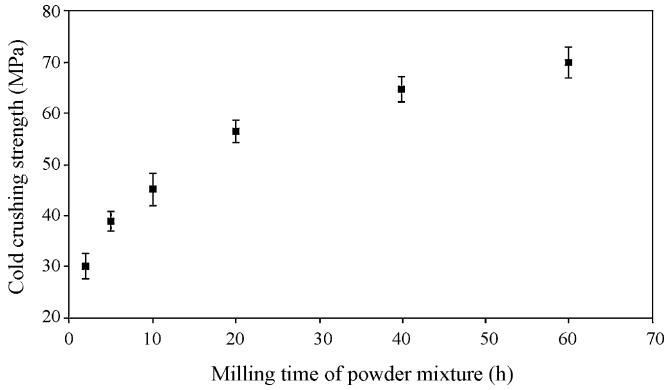

Fig. 6. Mechanical properties of sintered magnesium aluminate spinels as a function of milling time of the initial powder mixture.

interface of the reacting phases, which may enhance the reaction kinetics during the subsequent annealing. After 5 h of mechanical activation and subsequent annealing at 1200 °C for 1 h, only the spinel phase can be detected on the XRD pattern. Further milling up to 60 h had no significant effects on structure or phase composition of the samples after the subsequent annealing. The absence of MgO and Al_2O_3 on the XRD patterns indicates that during mechanical activation, a homogeneous powder mixture was achieved. As can be seen in Fig. 4b, the intensity of XRD peaks decreased with increasing milling time, while their width increased after annealing at 1200 °C for 1 h. This is because the crystallite size after annealing is lower for samples milled for longer times (as shown in Fig. 5).

The crystallite sizes of the prepared spinel ceramic are shown in Fig. 5 as a function of ball milling time. As can be seen, by increasing the milling time from 2 to 60 h, the crystallite size after annealing decreased continuously from 45 to 25 nm. As milling proceeded, the density of dislocation increased as a result of more nucleation sites being available during crystallization upon annealing, which in turn led to the smaller final crystallite size [3].

3.3. Mechanical properties

Effect of ball milling period on cold crushing strength (CCS) of spinel samples is shown in Fig. 6. Generally, CCS increases with increasing milling time and there is a significant difference in the CCS of samples after 2 and 60 h of milling time as a result of decrease in the powder crystallite size after subsequent heat treatment. Another reason for this behavior is that more $MgCO_3$ particles were decomposed with increasing milling time, whereupon a lower amount of CO_2 was released from the bulk sample during the subsequent heat treatment which led to the higher density and lower porosity of the spinel bodies. The maximum strength of the fired spinel bodies was 70 MPa for the sample obtained from the powder mixture milled for 60 h. This finding is comparable to those reported by Zawrah et al. [17]. They reported that the cold crushing strength of spinel bodies after firing at 1550 °C for 2 h was about 65 MPa. Smaller crystallite sizes in the nano-range led to a significant reduction in the sintering temperature and to better mechanical properties.

3.4. SEM analysis

Fig. 7(a, c) and (b, d) shows the SEM micrographs of the samples milled for 5 and 60 h after annealing at 1200 °C for 1 h, respectively. As can be seen in Fig. 7a, the powder milled for 5 h consisted of very small and highly agglomerated particles with a rounded shape and agglomerate sizes smaller than 20 μm after subsequent annealing at 1200 °C for 1 h. The agglomerate of the spinel powder prepared by 60 h of ball milling and annealed for 1 h at 1200 °C was less than 20 μm with an irregular shape (Fig. 7b). The obtained spinel powder

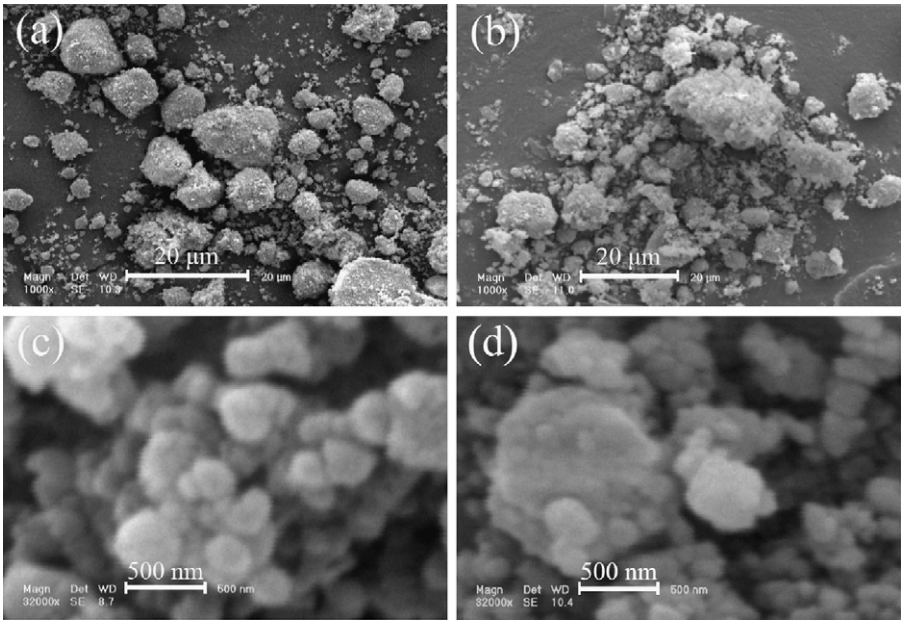

Fig. 7. SEM micrographs of (a and c) 5 h milled powders, and (b and d) 60 h milled powders after annealing at 1200 °C for 1 h.

after 5 h of milling and subsequent annealing at 1200 °C for 1 h had a particle size of less than 500 nm (Fig. 7c). As can be seen in Fig. 7d, with increasing the milling time, the particle size of powder milled for 60 h and then annealed at 1200 °C for 1 h was less than 200 nm.

4. Conclusion

Mechanical activation with subsequent annealing of $MgCO_3$ and Al_2O_3 led to the formation of the single-phase nanocrystalline spinel ($MgAl_2O_4$) powder. It is clear that ball milling activates the mixed particles, which is favorable for the solid-state reaction of the reactant particles forming the $MgAl_2O_4$ phase at a lower temperature. Liberation of CO_2 due to the decomposition of magnesium carbonate during the mechanical activation process led to increased contact surface area and better reactivity of initial materials after subsequent annealing. Single phase nanocrystalline spinel powder was synthesized for 5–60 h of mechanical activation with subsequent annealing at 1200 °C for 1 h. The crystallite size of the prepared spinel phase was between 25 and 45 nm. By decreasing the crystallite size as a result of increasing milling time, the cold crushing strength increased. The maximum cold crushing strength obtained was 70 MPa for the sample prepared from the powder mixture milled for 60 h.

References

[1] B. Alinejad, H. Sarpoolaky, A. Beitollahi, A. Saberi, S. Afshar, Mater. Res. Bull. 43 (2008) 1188–1194.
[2] A. Saberi, F. Golestani-Fard, M. Willert-Porada, Z. Negahdari, C. Liebscher, B. Gossler, Ceram. Int. 35 (2009) 933–937.
[3] F. Tavangarian, R. Emadi, J. Alloys Compd. 485 (2009) 648–652.
[4] C. Suryanarayana, Prog. Mater. Sci. 46 (2001) 1–184.
[5] F.H. Froes, O.N. Senkov, E. Baburaj, Mater. Sci. Eng. A 301 (2001) 44–53.
[6] D. Mohapatra, D. Sarkar, J. Mater. Sci. 42 (2007) 7286–7293.
[7] J. Salmones, J.A. Galicia, J.A. Wang, M.A. Valenzuela, G. Aguilar-Rios, J. Mater. Sci. Lett. 19 (2000) 1033–1037.
[8] R. Smith, D. Bacorisen, B.P. Uberuaga, K.E. Sickafus, J. Phys. Condens. Matter 17 (2005) 875–891.
[9] G. Baudin, R. Martinez, P. Pena, J. Am. Ceram. Soc. 78 (1995) 1857–1862.
[10] G. Cambaz, M. Timucin, Key Eng. Mater. 264 (2003) 1265–1268.
[11] C.W. Fairhurst, Adv. Dent. Res. 6 (1992) 78–81.
[12] L. Thomé, A. Gentils, J. Jagielski, F. Garrido, T. Thomé, Vacuum 81 (2007) 1264–1270.
[13] S.A. Bocanegra, S.R. de Miguel, A.A. Castro, O.A. Scelza, Catal. Lett. 96 (2004) 129–140.
[14] W. Glaubitt, W. Watzka, H. Scholz, D. Sporn, J. Sol–Gel Sci. Technol. 8 (1997) 29–33.
[15] V. Singh, R.P.S. Chakradhar, J.L. Rao, D.K. Kim, J. Solid State Chem. 180 (2007) 2067–2074.
[16] L.F. Koroleva, Glass Ceram. 61 (2004) 299–302.
[17] M.F. Zawrah, H. Hamaad, S. Meky, Ceram. Int. 33 (2007) 969–978.
[18] N. Yang, L. Chang, Mater. Lett. 15 (1992) 84–88.
[19] S.K. Behera, P. Barpanda, S.K. Pratihar, S. Bhattacharyya, Mater. Lett. 58 (2004) 1451–1455.
[20] H. Zhang, X. Jia, Z. Liu, Z. Li, Mater. Lett. 58 (2004) 1625–1628.
[21] T. Shiono, K. Shiono, K. Miyamoto, J. Am. Ceram. Soc. 83 (2000) 235–237.
[22] C.X. Huang, Z.X. Peng, Y.P. Wang, J. Synth. Cryst. 25 (1996) 108–114.
[23] C.R. Bickmore, K.F. Waldner, D.R. Treadwell, J. Am. Ceram. Soc. 79 (1996) 1419–1423.
[24] C.T. Wang, L.S. Lin, S.J. Yang, J. Am. Ceram. Soc. 75 (1992) 2240–2243.
[25] V. Montouillour, D. Massior, A. Douy, J. Am. Ceram. Soc. 82 (1999) 3299–3304.
[26] K. Hamano, Z. Nakagawa, T. Kanai, V. Ohya, M. Hasegawa, Report Res. Lab. Eng. Mater., Tokyo Inst. Technol. 11 (1986) 93–101.
[27] S.A. Bocanegra, A.D. Ballarini, O.A. Scelza, S.R. de Miguel, Mater. Chem. Phys. 111 (2008) 534–541.
[28] K.J.D. Mackenzie, J. Temuujin, T.S. Jadambaa, M.E. Smith, P. Angerer, J. Mater. Sci. 35 (2000) 5529–5535.
[29] A.R. West, Solid State Chemistry and its Applications, John Wiley & Sons, 1984.
[30] G.K. Williamson, W.H. Hall, Acta Metall. 1 (1953) 22–31.
[31] M.A. Sainz, A.D. Mazzoni, E.F. Aglietti, A. Caballero, Mater. Chem. Phys. 86 (2004) 399–408.
[32] D. Domansky, G. Urretavizcaya, F. Castro, F. Gennari, J. Am. Ceram. Soc. 87 (2004) 2020–2024.
[33] S.J. Kiss, E. Kostić, D. Djurović, S. Bošković, Powder Technol. 114 (2001) 84–88.
[34] E. Kostic, S. Kiss, S. Boskovic, Powder Technol. 92 (1997) 271–274.
[35] C.A. Schacht, Refractories Handbook, CRC Press, 2004.